Canine Sternal Force-Displacement Relationship During Cardiopulmonary Resuscitation

Kreg G. Gruben,* *Member, IEEE*, Henry R. Halperin, *Member, IEEE*, Aleksander S. Popel, and Joshua E. Tsitlik, *Senior Member, IEEE*

***Abstract*— A viscoelastic model developed to model human sternal response to the cyclic loading of manual cardiopulmonary resuscitation (CPR) [8] was used to evaluate the properties of canine chests during CPR. Sternal compressions with ventilations after every fifth compression were applied to supine canines $(n = 7)$ with a mechanical resuscitation device. The compressions were applied at a nominal rate of 90/min with a peak force near 400 N. From measurements of sternal force, sternal displacement, and tracheal airflow, model parameters were estimated and their dependence on time and lung volume evaluated. The position to which the chest recoiled between compressions changed with time at a mean rate of 1.0 mm/min. Within each ventilation cycle (five compressions) the sternal recoil position decreased by 2.0 cm for each liter of decrease in lung volume. The elastic force and damping decreased with time and decreasing lung volume. Canine and human [8] model parameters were found to be similar despite the notable differences in thoracic anatomy between the species, supporting the continued use of canines as models for human CPR. These parameters may be useful in the development of a model relating sternal compression forces to blood flow during CPR.**

***Index Terms*—Biomechanics, canine, cardiopulmonary resuscitation, elasticity, human, model, thorax, viscosity.**

I. Introduction

MORE than 300 000 people die each year in the United States from cardiac arrest [1]. Cardiopulmonary resuscitation (CPR) improves the chances of survival by generating vascular pressure gradients which drive the flow of oxygenated blood to vital organs. The mechanisms by which these gradients are generated continue to be debated [2], [4], [5], [9], [10], [13], [15]. It is clear that the application of cyclic force to the sternum causes deformation of the thorax. The debate centers on just how this deformation generates pressures in the vascular spaces. Some argue that the heart is directly compressed by the sternum and vertebral column, while others cite evidence for a general rise in intrathoracic pressure. Models of CPR [3] continue to use pressure application to the heart and/or thoracic vessels as an input. However, since the dynamic behavior of the rib cage and lungs affects the transmission of sternal force into intrathoracic pressures, these models cannot be used to investigate the effectiveness of sternal force waveforms which is a principal variable over which the rescuer has control. A comprehensive model of CPR would require sternal force as input, thus requiring knowledge of the relationship between sternal force and displacement. The purpose of the present study is to summarize the relationship between the canine force and displacement during CPR with a simple phenomenological model which should prove useful in the development and evaluation of future models of CPR.

A model has been proposed which described the relationship between the sternal force and displacement for the human chest during actual resuscitation attempts [8]. Due to the difficulties of studying CPR directly in humans, much of CPR research has been conducted using canines [3]–[5], [9], [10]. Hemodynamic similarities between these species during CPR has been demonstrated [3], however, despite this widespread use of canines and the significant inter-species differences in thoracic anatomy, comparison of the thoracic mechanical properties during CPR has not been published.

A large body of literature exists which describes the behavior of the canine thorax during various manipulations. However, no descriptions were found which address the behavior of the sternum of an intact chest when subjected to posteriorly directed force oscillations at a frequency of 1.5 Hz and approximately 400 N magnitude, such as those typically used during CPR.

The objective of the present study was to quantify the dynamic relationship between sternal force and displacement during canine CPR. The model developed to represent human thoracic properties presented by Gruben *et al.* [8] was used to describe data acquired during mechanical CPR on canines. The sternal response properties of humans and canines were then compared and the dependence of the canine properties on lung volume and time were assessed. This analysis may help test the applicability of canine study results to the clinical environment.

II. Materials and Methods

The following experimental protocol was approved by the Animal Care and Use Committee of The Johns Hopkins

Manuscript received October 7, 1997; revised January 21, 1999. This work was supported in part by the National Heart, Lung, and Blood Institute, Bethesda, MD, under Grant RO1-38174 and Ischemic Heart Disease SCOR Grant 5P50-HL-17655, and by a grant from the Asmund Laerdal Foundation, Stavanger, Norway. *Asterisk indicates corresponding author.*

*K. G. Gruben is with the Department of Kinesiology, University of Wisconsin-Madison, Madison, WI 53706 USA (e-mail: gruben@soemadison @wisc.edu).

H. R. Halperin is with the Peter Belfer Cardiac Mechanics Laboratory, the Cardiology Division of the Department of Medicine and the Department of Biomedical Engineering at the Johns Hopkins University and Medical Institutions, Baltimore, MD 21287 USA.

A. S. Popel is with the Department of Biomedical Engineering at the Johns Hopkins University and Medical Institutions, Baltimore, MD 21205 USA.

J. E. Tsitlik is with ServiceMaster Management Services Company, Chicago, IL 60612 USA.

Publisher Item Identifier S 0018-9294(99)04694-7.

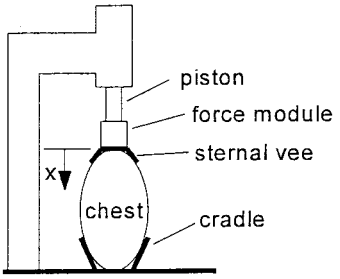

Fig. 1. Experimental setup. The supine canines were placed in a thoracic cradle and sternal compression was delivered through a sternal vee. These lateral supports ensured repeatable compressions by maintaining the canines supine position. The piston of a pneumatic chest compressor was connected to a force measuring module [7] which was in turn connected to the sternal vee. The cradle sides measured 46×8.4 cm and tilted 25° off vertical, while the sternal vee measured 4.2 cm along the canine's long axis by 5.6 cm, tilted 40° off vertical.

University, Baltimore, MD, and the care and handling of the animals were in accord with National Institutes of Health guidelines. Mongrel canines $(n = 7)$ with body mass between 21.8 and 26.8 kg (mean = 23.9 kg) were anesthetized with sodium pentobarbital (32 mg/kg iv) and additional dosage was administered as necessary. Mechanical volume ventilation was provided during preparation (Harvard Respiration Pump, model 607, Harvard Apparatus Co., Inc., Millis, MA). The canines were placed supine in a cradle and sternal compressions were applied through a rigid sternal vee whose purpose was to ensure repeatable application of compression force to the sternum. The sides of the sternal vee were of sufficient size to keep the chest compressor centered on the sternum while not being so large that lateral rib motion was impeded (Fig. 1). The sides of the thoracic cradle and sternal vee could slide laterally to accommodate variations in chest size and were fixed in place once being adjusted to ensure a snug fit against for each canine. Sternal compressions were performed by a mechanical pneumatic chest compression device modified by the manufacturer to be computer controlled (Fig. 1) ("Thumper," Life Aid Cardio Pulmonary Resuscitator, Model: X1004, Michigan Instruments, Inc., Grand Rapids, MI). The piston of this device was connected to a force measuring module [7] which was in turn attached to the sternal vee. This module measured only the vertical component of the sternal force. Sternal displacement was measured with a linear potentiometer (model: M1326-4-103, Maurey Instrumentation, Chicago, IL) attached to the sternal vee and a frame mounted to the surgical table.

Ventricular fibrillation was induced with 60-Hz alternating electrical current delivered to the right ventricle via a pacing catheter. Following fibrillation, sternal compressions were delivered once every 0.67 s (equivalent to a rate of 90 cycles/min). A Bear1 Adult Volume Ventilator (Bourns Medical Systems, Inc., Riverside, CA) modified to be externally controlled was used to ventilate the canine through a tracheostomy during chest compressions. Breaths of approximately 300 ml room air were delivered while compressions were suspended for 1.2 s following every fifth compression. A pneumotachometer (model: 3, S/N: 3.5926, Fleisch, Switzerland) coupled with a differential pressure transducer (model: DP45-22, S/N: 19150, Validyne Engineering Corp., Northridge, CA) was connected in the ventilation line for measurement of tracheal airflow.

Force (F), displacement (x), and airflow (Q) measurements were digitized at a rate of 200 Hz and recorded on magnetic disk for subsequent analysis. Velocity $(\dot{x})$ was calculated from displacement using a two-point centered derivative and was then digitally filtered (2 dB cutoff frequency = 18 Hz). Acceleration was calculated by taking the first time derivative of the filtered velocity. The force applied to the sternum was calculated by subtracting the product of the acceleration and the mass of the sternal vee (mass = 0.475 kg) from the measured force. The zero displacement position was taken as the minimum value for displacement for each canine's data set. Force and displacement are expressed in Newtons (N) and centimeters (cm), respectively, with velocity in units of centimeters per second (cm/s). Airflow is expressed in liters/second (l/s) and lung volume in liters (l).

Segments of data 90 s long were selected for analysis. This length of data was chosen to ensure that enough compression cycles would be observed to accurately represent the chest properties and to adequately assess the dependence of these properties on time and lung volume. All canines received at least one minute of prior compressions to assure initial mechanical preconditioning of the chest. Due to the use of mechanical compression and ventilation devices the compressions were extremely repeatable (Fig. 2). This allowed analysis of the effects of time and lung volume on the mechanical response of the sternum.

The data were summarized using the model developed for human sternal response properties during CPR reported in a previous paper [8]

$$F = F^e + F^d + \epsilon \tag{1}$$

where

$$F^e = a_0 + a_1 x + a_2 x^2 + a_3 x^3 + a_4 x^4 \tag{2}$$

$$F^d = \mu \dot{x} \tag{3}$$

$$\mu = d_1 + d_2 x \tag{4}$$

F^e, the elastic force, represents a nonlinear spring, and F^d, the damping force, represents a viscous element with displacement-dependent effective viscosity μ, and ϵ is the error. A fourth-order polynomial was selected for the elastic force since it caused a significant reduction in systematic error over a third-order and a fifth-order did not significantly reduce the error.

This model differs slightly from that given in [8] in that here a_0 is a force offset rather than a displacement offset. This was chosen because the mechanical compression device used in this study did not return completely to a zero force level after every compression as did the manual compressions used in the human studies [8]. The model parameters $(a_0, \cdots, a_4, d_1, d_2)$ were estimated for each compression cycle separately using standard linear regression [16].

Due to the highly correlated nature of the polynomial parameters (a_i), the elastic force (F^e) reconstructed from

these parameters was also represented by a four-segment linear spline [8] whose parameters are more independent:

$$\tilde{F}^e = \begin{cases} k_0 + k_1 x, & \text{when } 0 \le F^e < 20\text{N} \\ 20 + k_2(x - x_1), & \text{when } 20 \le F^e < 100\text{N} \\ 100 + k_3(x - x_2), & \text{when } 100 \le F^e < 300\text{N} \\ 300 = k_4(x - x_3), & \text{when } 300 \le F^e. \end{cases} \quad (5)$$

Here $x_1 = (20 - k_0)/k_1, x_2 = x_1 + 80/k_2$, and $x_3 = x_2 + 200/k_3$. These elastic spline parameters k_i ($I = 0$ to 4) provide an approximation of the chest's stiffness in the four force ranges. The elastic and damping properties at the lowest displacements are given by k_1 and d_1, respectively. The other elastic spline parameters describe the chest stiffness at higher displacements and the damping parameter d_2 describes the dependence of the damping on displacement. The procedure used to estimate the elastic spline parameters from the elastic polynomial parameters is described in the Appendix.

This results in a set of seven parameters $(k_0, k_1, k_2, k_3, k_4, d_1, d_2)$ for each compression cycle for each canine. These parameters change from cycle to cycle and in order to describe this variability, we introduce additional notation. The entire set of parameters for a single canine may be represented as $k_{0j}, k_{1j}, k_{2j}, k_{3j}, k_{4j}, d_{1j}, d_{2j}$ $(j = 1, 2, \cdots, 100)$. The index, j, is the compression cycle number.

Each compression cycle occurs at a particular time

$$t_j, j = 1, 2, \cdots, 100 \quad (6)$$

where t_j is the time at the beginning of each of the 100 compression cycles which were performed during the 90 s of acquired data (Fig. 2). This is the time elapsed since the beginning of the data set (i.e., $t_1 = 0$ s, $t_2 \approx 0.67$ s, $\cdots, t_6 \approx 4.55$ s, $\cdots$). The beginning of a compression cycle was defined as 0.05 s before the time of peak sternal velocity. This was used as a more reliable marker of the time in which sternal force begins to increase. Each data set consists of 100 compression cycles because this is the number that are contained in the analyzed 90 s data segment.

To quantify the degree of lung inflation at the beginning of each compression cycle we introduce the following:

$$V_j = \begin{cases} 0, & \text{when } j = 5n - 4 \\ V_{j-1} = \displaystyle\int_{t_{j-1}}^{t_j} Q\, dt, & \text{when } j \ne 5n - 4 \end{cases} \quad (7)$$

where V_j is the change in lung volume from the beginning of the first compression cycle in the current ventilation cycle to the beginning of the current compression cycle (Fig. 2). Here, n is the ventilation cycle number to which the jth compression cycle belongs $(n = 1, 2, \cdots, 20)$. For example, the first five compression cycles ($j = 1$, 2, 3, 4, 5) are part of the first ventilation cycle $(n = 1)$ and compression cycles 6–10 ($j = 6$, 7, 8, 9, 10) belong to the second ventilation cycle $(n = 2)$. Thus, the 100 compression cycles that occur in the 90 s of analyzed data, will contain 20 ventilation cycles.

To summarize the manner in which the lung volume changed with each of the five compressions of each ventilation cycle a further variable was calculated for each canine

$$\overline{V}_p = \frac{\displaystyle\sum_{i=1}^{20} V_{5(i-1)+p}}{20} \qquad p = 1, 2, 3, 4, 5. \quad (8)$$

Here $\overline{V}_p$ is the mean lung volume change at the beginning of each of the five compression cycles making up a ventilation cycle. Because V_j is zero for the first compression after a ventilation, $\overline{V}_p = 0$, and the rest are <0 because the lungs had a net loss of volume with each compression.

The dependence of the parameters $(k_{0j}, k_{1j}, k_{2j}, k_{3j}, k_{4j}, d_{1j}, d_{2j})$ on time and changes in lung volume was examined and was best described by the following equations:

$$\begin{aligned} k_{mj} &= \kappa_{0m} + \kappa_{1m} t_j + \kappa_{2m} V_j, \qquad m = 0, 1, 2, 3, 4 \\ d_{mj} &= \delta_{0m} + \delta_{1m} t_j + \delta_{2m} V_j, \qquad m = 1, 2. \end{aligned} \quad (9)$$

Standard least squares regression was used to estimate the parameters $(\kappa_{0m}, \kappa_{1m}, \kappa_{2m}, \delta_{0m}, \delta_{1m}, \delta_{2m})$ for each canine. These parameters have the following interpretation: κ_{0m} is the estimated value of the parameter k_m at the beginning of the data set $(t_1 = 0)$ and at the beginning of ventilation cycle $(V_j = 0)$, i.e., just after the inflation of the lungs; κ_{1m} describes the dependence of the parameter k_m on time once the dependence on lung volume has been accounted for; and κ_{2m} describes the dependence of the parameter k_m on lung volume once the dependence on time has been accounted for. Similarly for the δ parameters.

The position to which the chest recoils when applied force is at a minimum just before each compression will be called the minimum displacement $(x_j^{\min})$ for that compression. This value changes through the duration of CPR and is also dependent on the volume of air in the lungs. To quantify these relationships the following equation was used:

$$x_j^{\min} = \gamma_1 t_j + \gamma_2 V_j \qquad j = 1, 2, \cdots, 100. \quad (10)$$

The parameter γ_1 indicates the rate at which the minimum displacement changes with time and the parameter γ_2 indicates the effect of lung volume on the sternal position.

Student's t distribution [16] was used in all statistical tests.

III. Results

Sample data showing two complete ventilation cycles and the associated ten compression cycles from one of the canines is displayed in Fig. 2. Sternal force and displacement, tracheal airflow and lung volume change as well as the difference between the measured force and that predicted from the model are all plotted versus time. The dynamic relationship between the force and displacement can be more easily visualized in a plot of force versus displacement [Fig. 2(lower panel)]. For each canine the maximum force, maximum displacement, and maximum absolute velocity were calculated and are summarized here: 410 ± 18.4 N, 4.22 ± 0.426 cm, and 60.0 ± 7.49 cm/s (mean $\pm$ standard deviation, $n = 7$), respectively. The force required to accelerate the sternal vee during its largest acceleration was approximately 10 N, which is 2.5% of the

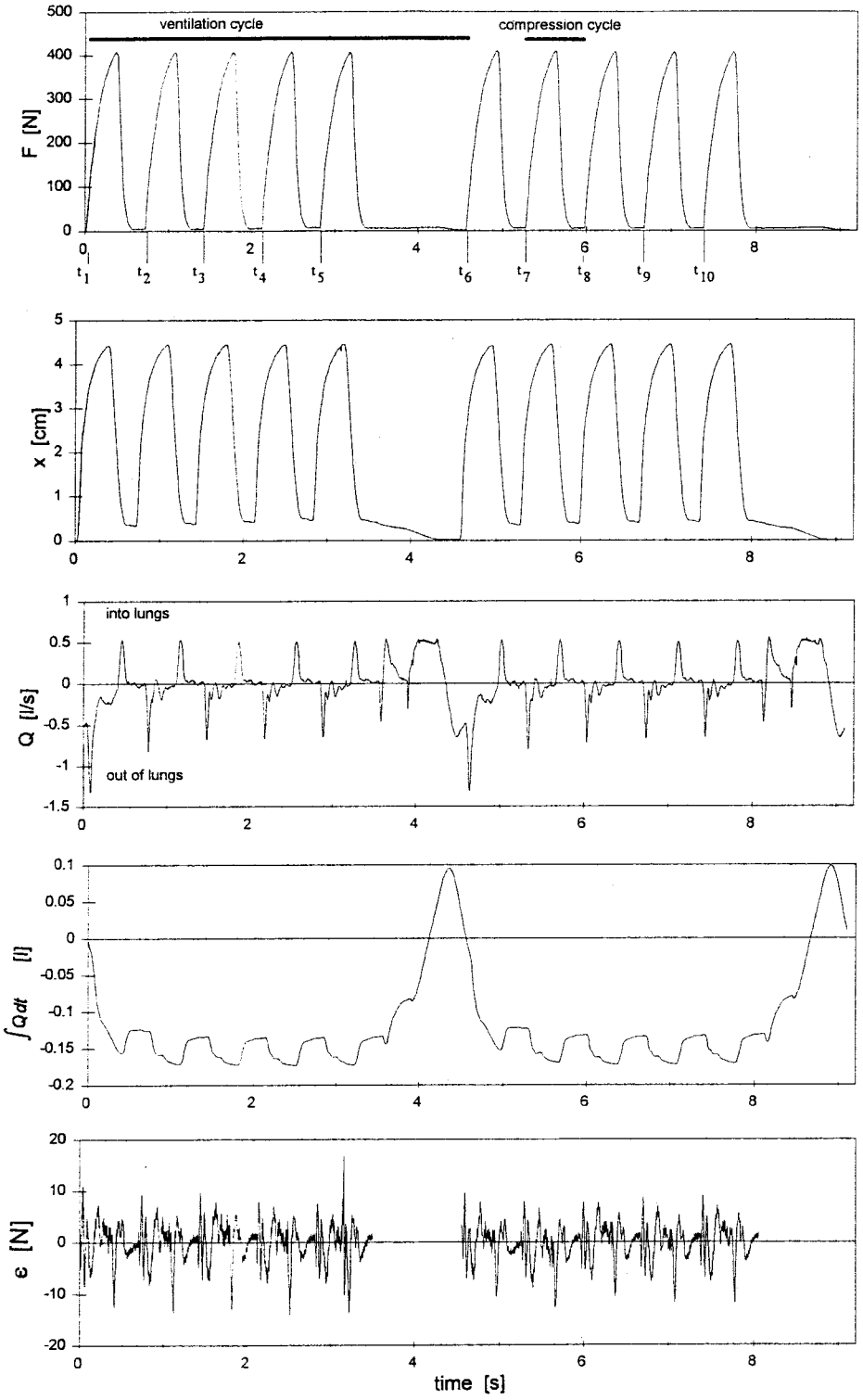

(a)

Fig. 2. Sample data. (a) These measurements of sternal force (F) and displacement (x), and tracheal airflow (Q) are a subset of the analyzed data from canine #4. A compression cycle (upper panel) begins 0.05 s before the point of maximum sternal velocity and continues until the beginning of the next cycle except for the fifth cycle after a ventilation which is the same length as the other cycles ($\approx$0.67 s). A ventilation cycle (upper panel) consists of five compression cycles followed by a ventilation for a total duration of $\approx$4.55 s. The fourth panel shows the change in lung volume which is calculated by integrating the air flow in the third panel. The fifth panel displays the error (ϵ) which is the difference between the measured force and that predicted from the model.

maximum force applied to the sternum. This peak acceleration occurs at the beginning of the compression cycle and is of brief duration, its rise from zero and return to zero lasting approximately 50 ms.

The ability of the model to describe the data can be assessed by considering the error plotted in Fig. 2 (fifth panel). The magnitude of this error is quantified by the coefficient of determination [8] r^2, which had a minimum value of 0.997

TABLE I
PARAMETER ESTIMATES. (a) MEAN PARAMETER VALUES FOR ALL CANINES, (b) MEAN PARAMETER VALUES FOR ALL CANINES EXCEPT #1, AND (c) PARAMETER UNITS

	m				
parameter	0	1	2	3	4
κ_{0m}	−3.63	31.5	63.5	143	227
κ_{1m}	−0.0518	0.00349*	−0.0115*	−0.0172*	0.141
κ_{2m}	44.9	−9.72*	9.24*	−65.6	−193*
δ_{0m}		0.497	0.852		
δ_{1m}		−0.001706	0.0000166*		
δ_{2m}		2.76	−0.0604		
γ_1	0.00164				
γ_2	−2.60				

(a)

	m				
parameter	0	1	2	3	4
κ_{0m}	−3.37	31.6	62.4	144	228
κ_{1m}	−0.0496	0.00728†	−0.0160†	−0.0250†	0.114
κ_{2m}	23.1	1.20†	1.11†	−37.6	−83.8
δ_{0m}		0.424	0.840		
δ_{1m}		−0.00142	−0.000103†		
δ_{2m}		1.70	−0.0739		
γ_1	0.00164				
γ_2	−2.60				

(b)

	m				
parameter	0	1	2	3	4
κ_{0m}	N	N/cm	N/cm	N/cm	N/cm
κ_{1m}	N/s	N/(cm · s)	N/(cm · s)	N/(cm · s)	N/(cm · s)
κ_{2m}	N/1	N/(cm · 1)	N/(cm · 1)	N/(cm · 1)	N/(cm · 1)
δ_{0m}		N · s/cm	N · s/cm^2		
δ_{1m}		N/cm	N/cm^2		
δ_{2m}		N · s/(cm·1)	N · s/(cm^2·1)		
γ_1	cm/s				
γ_2	cm/1				

(c)

* Not significantly different than zero ($p < 0.05, n = 7$).
† Not significantly different than zero ($p < 0.05, n = 6$).

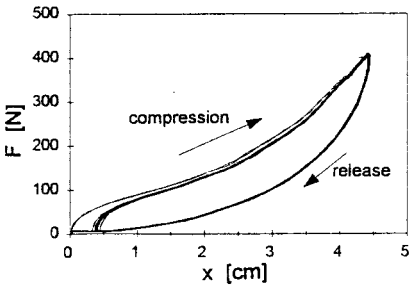

(b)

Fig. 2. (*Continued*). (b) Force versus displacement loops are traversed in a clockwise manner illustrating the dynamic relationship between these measurements. This panel illustrates the high degree of repeatability which is representative of all the data acquired.

indicating that most of the variation in the force has been described by the model.

Mean values over the seven canines of the κ and δ parameter estimates are presented in Table I(a). Canine #1 had κ_{2m} and δ_{2m} values (excluding δ_{22}) which were significantly different than the mean of the other canines ($p < 0.0001$) and thus was excluded from the mean parameters given in Table I(b). The κ_{0m} and δ_{0m} values are interpreted as the representative estimates of k_m and d_m, respectively, for the first compression of a ventilation cycle. The κ_{1m} and δ_{1m} values indicate the dependence of the parameter estimates on time, while the κ_{2m} and δ_{2m} values indicate the dependence on lung volume. The values which were not significantly different than zero are indicated in the table.

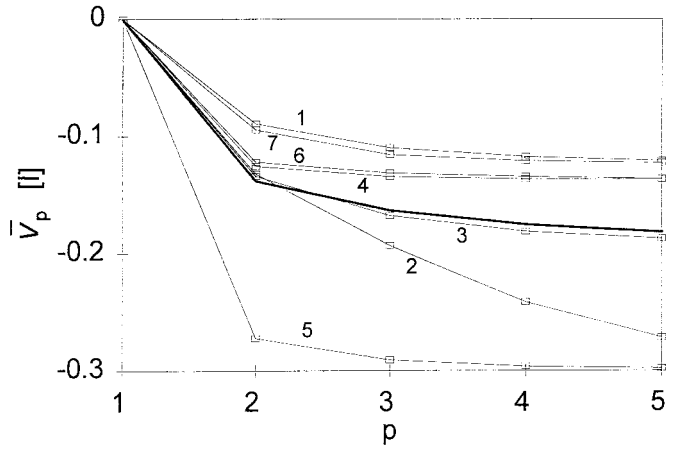

Fig. 3. Lung volume change. The change in lung volume $\overline{V}_p$ [see (8)] is plotted here versus compression cycle number p, within the ventilation cycle. Each line represents the data from an individual canine (identified by number), and the heavy line is the mean of the seven canines.

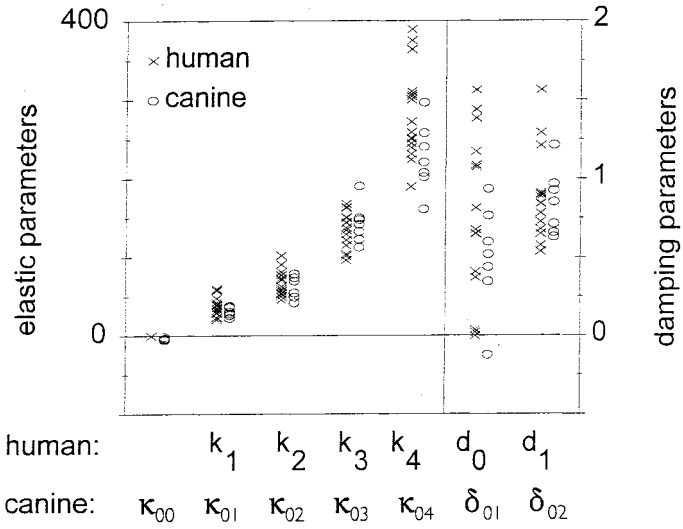

Fig. 4. Canine–human parameter comparison. The human parameters from a previous paper [8] along with the equivalent canine parameters from this study are presented graphically. The values used for the canines are the κ_{0m} and δ_{0m} values which represent the first compression in a ventilation cycle. The elastic spline parameters are on the left and the damping parameters are on the right. The similarity in both the mean and the variation of each of the parameters is evident. Only the parameter κ_{04} (k_4 for humans) was significantly different between the humans and the canines ($p < 0.025$). The units for the parameters are given in Table I(c).

The manner in which lung volume changed with compressions is illustrated in Fig. 3. As expected, the greatest change occurs with the first compression although the second and third compression also significantly reduce the volume. By the fourth compression the lung volume has nearly reached a steady state except in canine #2.

In order to compare the sternal response properties of humans and canines, κ_{0m} and δ_{0m} were chosen as parameters representative of each canine. These are compared graphically with the corresponding human parameters [8] in Fig. 4. Only the κ_{04} (k_4 for humans) parameter was significantly different ($p < 0.025$), with the humans being slightly higher indicating a stiffer chest at higher displacements.

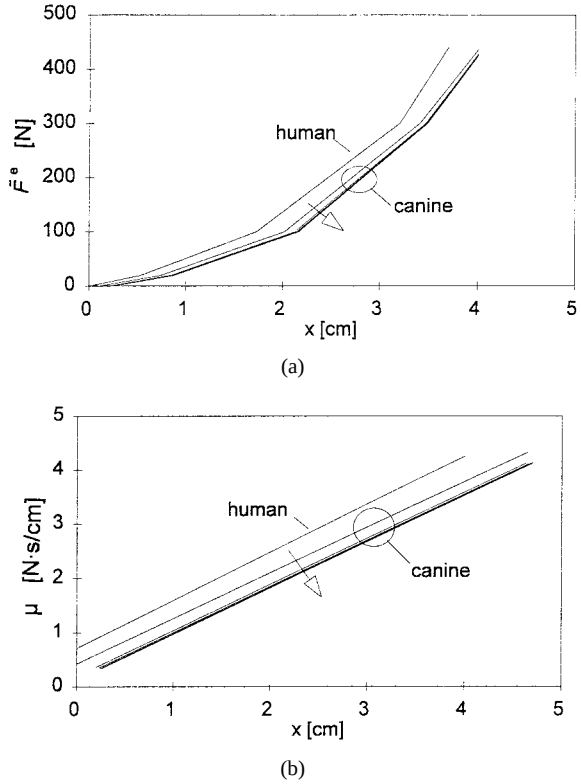

Fig. 5. Canine–human mechanical properties comparison. The elastic force [F^e, see (5)] curves calculated from the canine and human mean values (Table I(b) and [8]) are plotted versus displacement in the upper panel. The damping parameters are represented in the lower panel in plots of damping coefficient (Pμ) [see (4)] versus displacement. The five canine curves correspond to the five compressions in a ventilation cycle with the arrows indicating the progression from cycle one to five.

To represent a typical human the following values were used ($k_0 = 0$ N, $k_1 = 37.4$ N/cm, $k_2 = 66.8$ N/cm, $k_3 = 136$ N/cm, and $k_4 = 282$ N/cm [8]). To calculate canine parameters for each of the five compression cycles in a ventilation cycle the following equations were used.

$$k_{mp} = \kappa_{0m} + \kappa_{2m}\overline{V}_p, \qquad m = 0,1,2,3,4 \quad p = 1,2,3,4,5$$
$$d_{mp} = \delta_{0m} + \delta_{2m}\overline{V}_p, \qquad m = 1,2 \quad p = 1,2,3,4,5 \qquad (11)$$

where p is the compression cycle number within a ventilation cycle. These values were used in (5) and (4) to create the curves shown in Fig. 5. These lines represent the elastic and damping properties of the chests. The multiple curves shown for the canine reflect the influence of lung volume. The progression from compression one to five within the ventilation cycle is indicated by the arrows.

IV. Discussion

This study characterized the dynamics of the canine sternum during laboratory mechanical CPR using a model developed to describe the dynamics of the human sternum during clinical manual CPR. The model is viscoelastic in nature and the elastic element becomes more stiff while the viscous element becomes more viscous with increasing displacement. This model was able to describe the canine data as well as it did the human data and the mechanical parameters characterizing the two species

were similar. Similarity between human and canine thoracic mechanical behavior has also been reported by Kikuchi *et al.* [11], though their study involved the isolated canine rib cage.

The mechanical properties of biological tissues are known to vary with the frequency at which they are perturbed. Since the force waveform applied to the sternum during this study was stereotypical of those used during CPR, the properties found in this study are applicable to the study of CPR mechanics, but should not be generalized to all frequencies.

The position to which the chest recoils when force is removed $(x^{\min})$ varied during the course of compressions on each canine. Likely causes were lung air volume changes, blood volume shifts, and changes in chest material properties. During a ventilation cycle the recoil position increased with each compression, failing to return to the starting point of the previous compression (Fig. 2). A ventilation then restored the recoil position to near its initial position. This position $(x^{\min})$ was inversely related to changes in lung volume (Table I, γ_2) (Fig. 3). In addition to this variation, there was also a tendency for $x^{\min}$ to increase with time (Table I, γ_1). It was not possible in this study to distinguish whether it was changes in material properties or a slow decrease in lung volume or thoracic blood volume which was responsible for this behavior, though it seems likely that all may have contributed. The reason that this could not be discerned from the present data is discussed later.

The κ_{2m} and δ_{2m} parameter estimates (excluding δ_{22}) for canine #1 were significantly different than the mean of the other canines. All other data from this canine appeared unremarkable and the reason for this canines unusual relationship with lung volume changes could not be discerned. This prompted the exclusion of this canine in the creation of Table I-B in order to provide a more reliable summary of the canine parameters. Thus, the principal difference between Table I(a) and (b) occurs in these parameters.

The parameters displayed graphically in Fig. 4 show a great degree of overlap between the humans and canines. The similarity in location and variability of the values is apparent. Comparison of the elastic spline and damping parameters between canines and humans indicated no significant difference except in the parameter κ_{04}. This is evident in Fig. 5 where it can be seen that the curves are nearly parallel with the exception of the upper segment of the elastic spline. Despite the canine curves being consistently lower than the humans in Fig. 5, the variation among individuals in both populations is large enough that this difference is not significant.

The estimate of κ_{00} is less than zero (Table I and Fig. 4) due to the use of a linear spline to approximate a polynomial curve which approaches zero force at low displacements. Thus, this is an artifact of the linearization and not actual negative force. Likewise, one canine had some nonlinearity in its viscous behavior which resulted in a negative δ_{01} value (Fig. 4). This gave a negative damping coefficient for only a small fraction of the compression cycle because of the damping coefficient's dependence on displacement.

The parameters in Table I indicate that as time progressed the elastic force and damping decreased $(\kappa_{10}, \delta_{11})$ and there was a slight increase in the elastic stiffness at the highest displacements (κ_{14}). Once again it is not possible to distinguish whether these were the result of tissue conditioning, a slow change in lung volume, or some other effect.

The analysis of lung volume effects used the change in lung volume rather than the absolute lung volume for three reasons. 1) The change in lung volume was calculated by integration of air flow and any small errors in the zero level of the air flow signal would accumulate yielding large errors in volume after many cycles. Thus, the volume was zeroed at the beginning of each ventilation cycle. 2) To evaluate how lung volume affected the changes in mechanical parameters it was not necessary to measure the total lung volume but only the relative changes in volume. 3) The greatest changes in lung volume took place during each compression cycle and during ventilation itself. Whatever change in lung volume took place over many ventilation cycles was likely to be small compared to the compression cycle changes and would have been difficult to measure without more sophisticated measurement systems. In the analysis done here, such changes are lumped into the time-dependence terms $(\kappa_{1m}, \delta_{1m})$ in equation nine which takes into account lung volume changes over time as well as other time-dependent changes in tissue elasticity and damping.

The elastic force decreased with each compression during a ventilation cycle as evidenced by the curves in Fig. 5 and the κ_{20} values in Table I. The stiffness of the chest at the highest displacements increased through the ventilation cycle (κ_{23} and κ_{24}, Table I, Fig. 5). The damping coefficient decreased through the ventilation cycle though its dependence on displacement remained unchanged (δ_{21} and δ_{22}, Table I, Fig. 5). This effect of the lung volume on the mechanical properties of the chest was consistent across all the canines studied.

The model presented here contains a damping term which increases with compression of the chest. Since much of this damping was hypothesized to come from the motion of the abdominal and thoracic viscera whose effect on the sternal mechanics may be augmented with depth of sternal displacement, the present model was formulated with a damping coefficient which varied with sternal *displacement* rather than *force*. However, due to the forcing function used here it was not possible to distinguish whether the changes in the damping varied with force or displacement. Thus, the important aspect of the damping in this model is that it increases with compression of the chest, which may be a stress- or strain-related phenomenon.

One of the unique aspects of the model presented here is its displacement-dependent damping. The elastic portion of this model could also be considered dependent on displacement as the stiffness increases with displacement. Thus, *both* the elastic and damping properties increase with displacement. A model applied to various thoracic tissues in which the elastic and damping properties varied together and seem to be coupled has been reported by others [11], [6], [12]. The parameter used by these authors to relate the elastic and damping properties, hysteresivity (η), was calculated according to (12)

$$\eta = \frac{1.5 \text{ cycle}}{\text{s}} \cdot \frac{2\pi \text{ rad}}{\text{cycle}} \cdot \frac{\mu}{k}. \tag{12}$$

For each of the four spline force ranges the hysteresivity was calculated using the average canine values from Table 1-B. The

values varied from 0.14–0.23 which fall in the range of values reported by Kikuchi [11]. Despite significant differences in the form of these models they both may be attempting to describe a common behavior.

The phenomenological model of sternal dynamics presented here provides a characterization of both the human and canine chest which may be useful in further modeling of manual CPR. The elastic properties of the chests were found to be highly nonlinear while the damping properties were augmented by a linear function of displacement. The similarity of the thoracic mechanical properties of the two species was remarkable considering the differences in thoracic anatomy. The manner in which sternal forces produce intrathoracic pressures is dependent on the mechanical properties of the thorax. This study provides direct quantitative evidence that the canine and human chests respond similarly to sternal compressions and thus supports the continued use of canines as models for human CPR.

APPENDIX
Estimation of Elastic Spline Parameters

After the elastic polynomial parameters were estimated, the elastic force was calculated and used in the estimation of the elastic spline parameters. The elastic spline parameters were not estimated directly from the data because the nonphysiological discontinuities in the spline would bias the estimation of the damping parameters. The elastic spline parameters were estimated for each canine by first calculating F^e (from the estimated a_i) at each of 100 evenly spaced displacement values within the valid displacement range for each compression cycle. This set of displacement (x_i) and elastic force $[F^e(x = x_i)]$ values represents the elastic force curve as modeled with the fourth order polynomial (2). The four segment linear spline which best fit this data was determined by estimating the spline parameters with the Levenberg–Marquardt nonlinear regression algorithm (15) which minimized the expression below

$$\sum_{i=1}^{100} \left[\tilde{F}^e(x = x_i) - \left(a_0 + a_1 x_i + a_2 x_i^2 + a_3 x_i^3 + a_4 x_i^4\right)\right]^2. \tag{13}$$

REFERENCES

[1] *Textbook of Advanced Cardiac Life Support*, 2nd ed. Dallas, TX: American Heart Association, 1987, pp. 1–3.

[2] C. F. Babbs, and K. Thelander, "Theoretically optimal duty cycles for chest and abdominal compression during external cardiopulmonary resuscitation," *Acad. Emerg. Med.*, vol. 2, pp. 698–707, 1995.

[3] N. C. Chandra, J. E. Tsitlik, H. R. Halperin, A. D. Guerci, and M. L. Weisfeldt, "Observations of hemodynamics during human cardiopulmonary resuscitation," *Crit. Care Med.*, vol. 18, pp. 929–934, 1990.

[4] H. G. Deshmukh, M. H. Weil, C. V. Gudipati, R. P. Trevino, J. Bisera, and E. C. Rackow, "Mechanism of blood flow generated by precordial compression during CPR, I. studies on closed chest precordial compression," *Chest*, vol. 95, pp. 1092–1099, 1989.

[5] M. P. Feneley, G. W. Maier, J. W. Gaynor, S. A. Gall, J. A. Kisslo, J. W. Davis, and J. S. Rankin, "Sequence of mitral valve motion and transmitral blood flow during manual cardiopulmonary resuscitation in dogs," *Circ.*, vol. 76, pp. 363–375, 1987.

[6] J. J. Fredberg, and D. Stamenović, "On the imperfect elasticity of lung tissue," *J. Appl. Physiol.*, vol. 67, pp. 2408–2419, 1989.

[7] K. G. Gruben, J. Romlein, H. R. Halperin, and J. E. Tsitlik, "System for mechanical measurements during cardiopulmonary resuscitation in humans," *IEEE Trans. Biomed. Eng.*, vol. 37, pp. 204–210, 1990.

[8] K. G. Gruben, A. D. Guerci, H. R. Halperin, A. S. Popel, and J. E. Tsitlik, "Sternal force-displacement relationship during cardiopulmonary resuscitation," *J. Biomech. Eng.*, vol. 115, pp. 195–201, 1993.

[9] H. R. Halperin, J. E. Tsitlik, A. D. Guerci, E. D. Mellitis, H. R. Levin, A.-Y. Shi, N. Chandra, and M. L. Weisfeldt, "Determinants of blood flow to vital organs during cardiopulmonary resuscitation in dogs," *Circ.*, vol. 73, pp. 539–550, 1986.

[10] H. R. Halperin, J. E. Tsitlik, R. Beyar, N. Chandra, and A. D. Guerci, "Intrathoracic pressure fluctuations move blood during CPR: Comparison of hemodynamic data with predictions from a mathematical model," *Ann. Biomed. Eng.*, vol. 15, pp. 385–403, 1987.

[11] Y. Kikuchi, D. Stamenović, and S. H. Loring, "Dynamic behavior of excised dog rib cage: Dependence on muscle," *J. Appl. Physiol.*, vol. 70, pp. 1059–1067, 1991.

[12] T. Nicolai, C. J. Lanteri, and P. D. Sly, "Inherent coupling of elastic and dissipative behavior of the lung through a viscoelastic time constant," *J. Appl. Physiol.*, vol. 74, pp. 2358–2364, 1993.

[13] N. A. Paradis, B. G. Martin, M. G. Goetting, J. M. Rosenberg, E. P. Rivers, T. J. Appleton, and R. M. Nowak, "Simultaneous aortic, jugular bulb, and right atrial pressures during cardiopulmonary resuscitation in humans: Insights into mechanics," *Circ.*, vol. 80, pp. 361–368, 1989.

[14] W. H. Press, B. P. Flannery, S. A. Teukolsky, and W. T. Vetterling, *Numerical recipes in C: The art of scientific computing*. New York: Cambridge Univ. Press, 1990, pp. 542–547.

[15] M. L. Weisfeldt and H. R. Halperin, "Cardiopulmonary resuscitation: Beyond cardiac massage," *Circ.*, vol. 74, pp. 443–448, 1986.

[16] R. J. Wonnacott and T. H. Wonnacott, *Introductory Statistics*. New York: Wiley, 1985, pp. 228–240, 595–596.

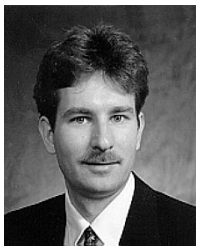

Kreg G. Gruben (S'89–M'91) received the B.S. degree in agricultural engineering from the University of Illinois, Urbana, in 1985 and the Ph.D. degree in biomedical engineering from The Johns Hopkins University, Baltimore, MD, in 1993, followed by a postdoctoral fellowship in surgical robotics at Johns Hopkins and IBM.

Since 1994, he has been an Assistant Professor in the department of Kinesiology at the University of Wisconsin-Madison. He is also affiliated with the departments of Biomedical Engineering and Mechanical Engineering. His research interests in the area of biomechanics currently entail the control of limb motion and the loading that results during constrained motion exercise.

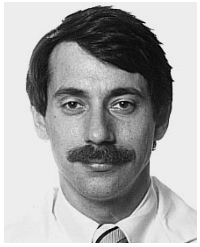

Henry R. Halperin (M'78) received the B.S. degree in physics with highest distinction from Purdue University, Lafayette, IN, in 1971. He received the M.A. degree in physics from the University of California, Berkeley, in 1972. He received the M.D. degree from Louisiana State University, New Orleans, in 1977.

He is currently an Associate Professor of Medicine and Biomedical Engineering at the Johns Hopkins Medical Institutions. He was a summer Research Assistant at Argonne National Laboratory, Argonne, IL and Lawrence Livermore Laboratory, Livermore, CA, in 1970 and 1971, respectively. He was a Medical Resident at Louisiana State University from 1977 to 1980, and a Fellow in Cardiology at The Johns Hopkins Hospital from 1981 to 1984. He serves on the editorial board of the journal *Resuscitation*, is a member of the national American Heart Association Advanced Cardiac Life Support Committee, and is the Director of the Johns Hopkins Hospital CPR team. He has over 100 publications and is co-editor of *Cardiac Arrest: The Science and Practice of Resuscitation Medicine* (Baltimore, MD: Williams and Wilkins, 1996). His current research interests include cardiopulmonary resuscitation, electrophysiology, and magnetic resonance imaging.

Dr. Halperin is a member of Phi Beta Kappa, an Established Investigator of the American Heart Association, and a McClure Fellow of The Johns Hopkins University Applied Physics Laboratory.

Aleksander S. Popel received the M.S. and Ph.D. degrees in mechanics at Moscow University, Moscow, Russia.

He served on the faculty at Tulane University, New Orleans, LA, University of Arizona, Tucson, and University of Houston, Houston, TX. He is currently a Professor in the Department of Biomedical Engineering, The Johns Hopkins University, Baltimore, MD, and Director of the Center for Computational Medicine and Biology. His research interests include biomechanics, biological transport, microcirculation, cell mechanics, and mathematical and computational modeling of biological systems. He is the author and co-author of 120 articles and book chapters and co-editor of two books.

Joshua E. Tsitlik (M'77–SM'83) received the M.S. and Ph.D. degrees in electrical engineering from Leningrad Polytechnical Institute, Leningrad, USSR, in 1964 and 1972, respectively, and the M.S. degree in clinical engineering from The Johns Hopkins School of Medicine, Baltimore, MD, in 1980.

From 1977 to 1995, he was with The Johns Hopkins School of Medicine; his last appointment was an Associate Professor of Medicine and Biomedical Engineering. From 1996 to 1998, he was affiliated with the start-up medical device companies. He is currently with ServiceMaster Management Services Company as an Associate Director for Technical Support of the Clinical Engineering Department in Cook County Hospital, Chicago, IL.